ARMY RESEARCH LABORATORY

Wind Profiles in Gentle Terrains and Vegetative Canopies for a Three-Dimensional Wind Field (3DWF) Model

by Yansen Wang and Ronald Cionco

ARL-TR-4178 July 2007

NOTICES

Disclaimers

The findings in this report are not to be construed as an official Department of the Army position unless so designated by other authorized documents.

Citation of manufacturer's or trade names does not constitute an official endorsement or approval of the use thereof.

Destroy this report when it is no longer needed. Do not return it to the originator.

Army Research Laboratory
Adelphi, MD 20783-1197

ARL-TR-4178 **July 2007**

Wind Profiles in Gentle Terrains and Vegetative Canopies for a Three-Dimensional Wind Field (3DWF) Model

Yansen Wang and Ronald Cionco
U.S. Army Research Laboratory
Computational and Information Sciences Directorate

REPORT DOCUMENTATION PAGE

Form Approved
OMB No. 0704-0188

1. REPORT DATE *(DD-MM-YYYY)*	2. REPORT TYPE	3. DATES COVERED (From - To)
July 2007	Final	

4. TITLE AND SUBTITLE
Wind Profiles in Gentle Terrains and Vegetation Canopies for a Three-Dimensional Wind Field (3DWF) Model

5a. CONTRACT NUMBER

5b. GRANT NUMBER

5c. PROGRAM ELEMENT NUMBER

6. AUTHOR(S)
Yansen Wang and Ronald Cionco

5d. PROJECT NUMBER

5e. TASK NUMBER

5f. WORK UNIT NUMBER

7. PERFORMING ORGANIZATION NAME(S) AND ADDRESS(ES)
U.S. Army Research Laboratory
Computational and Information Sciences Directorate
Battlefield Environment Division (ATTN: AMSRD-ARL-CI-EM)
Adelphi, MD 20783-1197

8. PERFORMING ORGANIZATION REPORT NUMBER
ARL-TR-4178

9. SPONSORING/MONITORING AGENCY NAME(S) AND ADDRESS(ES)
U.S. Army Research Laboratory
2800 Powder Mill Road
Adelphi, MD 20783-1197

10. SPONSOR/MONITOR'S ACRONYM(S)

11. SPONSOR/MONITOR'S REPORT NUMBER(S)
ARL-TR-4178

12. DISTRIBUTION/AVAILABILITY STATEMENT
Approved for public release; distribution is unlimited.

13. SUPPLEMENTARY NOTES

14. ABSTRACT
The objective of this study is to establish a simple wind profile parameterization for the U.S. Army Research Laboratory's (ARL) diagnostic Three-Dimensional Wind Field (3DWF) Model in gentle terrain and vegetation canopies. The Project Wind in Non-uniform Domains (WIND) data was applied for the analysis of wind profiles in open terrain, forest edge, and the interior of forest. A wind profile parameterization scheme was proposed according to this analysis and additional information found in the literature of other studies. The 3DWF simulation results using this scheme were compared with the observations to establish the confidence level of this parameterization. The analysis and comparison indicated that the 3DWF using this parameterization gives a reasonable accurate wind field prediction in a gentle terrain with vegetation environment. The application of the parameterization for different scenarios of data availability was also discussed.

15. SUBJECT TERMS
Diagnostic wind model, wind profile in vegetation, wind in complex terrain, wind data analysis

16. SECURITY CLASSIFICATION OF:			17. LIMITATION OF ABSTRACT	18. NUMBER OF PAGES	19a. NAME OF RESPONSIBLE PERSON
a. REPORT	b. ABSTRACT	c. THIS PAGE			Yansen Wang
U	U	U	SAR	40	19b. TELEPHONE NUMBER (*Include area code*) (301) 394-1310

Standard Form 298 (Rev. 8/98)
Prescribed by ANSI Std. Z39.18

Contents

List of Figures

List of Tables

Acknowledgment

The authors would like to thank Sam Chang of U.S. Army Research Laboratory for his helpful comments. The contributions in data collection by Army Dugway Proving Ground, USDA Forest Service, NOAA Air Resources Laboratory, and the University of Connecticut are also acknowledged.

1. Introduction

The 3-dimensional wind field (3DWF) is a simple, near real-time model and data assimilation system (*1, 2*). An initial wind field is required for a simulation in the 3DWF model and is adjusted with the mass conservation principle using a variational method to produce a mass-consistent diagnostic wind field. These initial wind profiles can be derived from several sources: in-situ wind sensor observations, remote sensor observations, or if the observation data are not available, the mesoscale weather forecast model output. The quality of the model results are closely related to the quality of the initial value.

Specifying proper initial vertical wind profiles for a microscale diagnostic wind model is difficult due to the complexity of the atmospheric boundary layer wind. Not only is the flow influenced by the larger scale weather systems, it is strongly modified by the surface roughness and thermal characteristics of the underlying surface. In the 3DWF model, many of the roughness and thermal effects are not explicitly resolved, but instead parameterized. This is because the diagnostic model seeks to quickly solve a wind field in real-time, and does not include momentum and thermal equations to explicitly resolve those variables. Several of the roughness and thermal effects on the atmospheric boundary layer wind can be parameterized in the initial wind field, assuming there are only small changes in the atmospheric variables in a short 5–10 min time frame. In the practice of meteorological modeling, unresolved physical processes are parameterized due to the spatial and temporal resolution issues and the computation power requirement. The parameterization approaches, such as the boundary layer, cloud processes, radiation, and land surface processes, have been used in mesoscale models. Parameterization of surface roughness and thermal effects in 3DWF is a useful solution.

An additional concern with the microscale model initialization involves the scarcity of data. In many situations, only a single-point observation is available. When this occurs, we must extrapolate the single point measurement of the entire model domain in a practical and logical manner. This requires determining the wind profile using information such as cloud coverage, atmospheric stability condition, the surface thermal property, and the morphological condition of the model domain. The extrapolated profile is usually the common or average profile based on observational results accumulated from the literature (*3, 4*).

The purpose of this report is to document a simple parameterization scheme for the 3DWF model to simulate wind over a gentle complex terrain and forest canopy, in a single point or single wind tower observation condition. In this case, the complex terrain has gentle slopes (<15°) and the local similarity theory can be approximately applied. The forest canopy patches are assumed to be large enough to occupy more than 5 by 5 grid points. This parameterization is based primarily on data obtained from Project Wind in Non-Uniform Domains (WIND) (*5*) orchard site, which had almost flat terrain with almond trees of uniformed size. Other more complex

issues are addressed in separate research efforts, for example, building wake and steep terrain parameterization, data assimilation using Doppler lidar wind, and an initialization model with mesoscale model output.

2. A Brief Description of Project WIND Orchard Site and Data

Project WIND (*5*) was conducted by U.S. Army laboratories and the U.S. Department of Agriculture Forest Service in and around the Sacramento River Valley of northern California, during 1985 to 1987. The data set analyzed in this report is from 1987 Project WIND, Phase IV, located on flat terrain northwest of Chico, CA. Figure 1 shows a schematic diagram of instrumentations and a 750 by 650 m aerial view of the entire 5,000 by 5,000 m experimental site. Fifty percent of the site is covered with almond orchard and 50% is cultivated field. The orchard is composed of mature 8 m tall trees planted on an 8 m square grid; the adjacent field is cut grain of uniform fetch. The three micrometeorological towers are identified as OT1 located in the cultivated field; OT2 located at the edge of the orchard; and OT3 located inside the orchard. OT1 was erected at >20 tree heights (tree height = 8 m) in the cultivated field and OT3 at 23 tree heights in the orchard. Eight levels of wind sensors (Gill UVW propeller anemometers), temperature, and relative humidity sensors were mounted at each tower as in the figure 1. Other instruments such as soil heat flux, solar radiation, sonic detection and ranging (SODAR), and radiosonde were used for upper air observations.

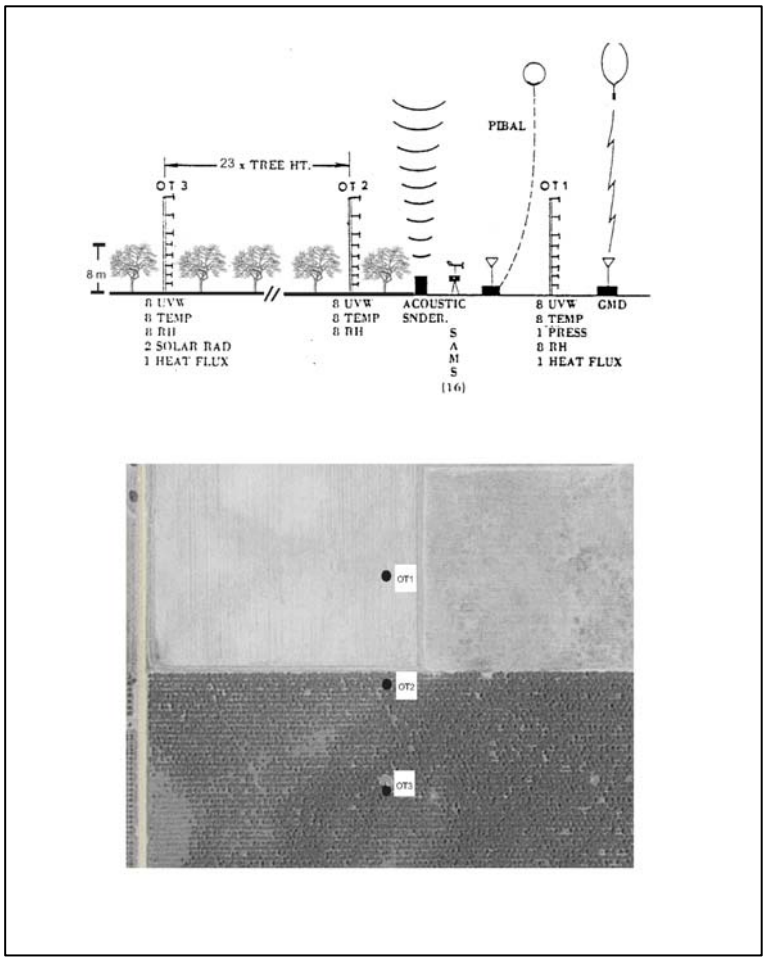

Figure 1. A schematic diagram across the orchard edge (top panel) and an aerial photograph (bottom panel) of the Project WIND orchard site.

The data we have analyzed in this report is shown in table 1. We have chosen samples of data according to wind flow directions in and out of the orchard edge. The different stability conditions were also sampled. Project WIND accumulated a large amount of micrometeorological data. We have analyzed a small portion of the data in a gentle terrain covered with forest canopy (orchard). The detailed description on the site and data is referred to in Cionc*o* (*5*).

Table 1. Sampled data set for wind profile analysis.

Date Julian Date (JD)	Time (PST)	Average Wind Direction	Wind Relative to the Orchard	Wind Speed at Canopy Height (m/s)	Stability Condition
9/26/1987 (JD269)	1100-1200	326	Flow into the edge	Strong, 8.5	Unstable
9/26/1987 (JD269)	1400-1500	320	Flow into the edge	Strong, 8.0	Unstable
9/25/1987 (JD268)	0000-0100	150	Flow out the edge	Moderate, 3.0	Stable
9/30/1987 (JD273)	1700-1730	280	Parallel to the edge	Weak, 1.2	Neutral
10/7/1987 (JD280)	0900-0930	170	Flow out the edge	Moderate, 3.6	Neutral

3. Wind and Temperature Profiles in a Gentle Terrain

In this section, the wind and temperature profile parameterizations over a gentle terrain are presented in three scenarios according to data availability. The first scenario is the data rich condition, where high frequency (10 Hz) temperature and wind data at different heights are available, and the turbulence momentum heat and momentum fluxes can be computed. The Monin-Obukhov (MO) Similarity Theory (*6*) can be directly applied using the observed values. The second scenario is where average temperatures and wind observations at different heights are available from slower sampled temperature and wind sensors. In this scenario, the stability parameters are estimated from the mean temperature gradients. The last scenario is when only a single point, slow response observation of wind and temperature is available. In this scenario, the wind profile was roughly approximated with a power exponential extrapolation, since other parameters, such as u_*, could not be estimated from single slow response sensor. Our primary focus in this report will be on the second and third scenarios, which require wind profile parameterization.

3.1 Data Rich Scenario: Multi-level High Frequency Data Availability

The surface layer wind profile over uniform terrain has been derived using the Kansas experiment data (*7, 8*). The flux-profile relationship is based on the MO Similarity Theory (*6*). This theory is based on an assumption of local equilibrium of turbulence production and dissipation; therefore, it is only suitable for the uniform or near uniform terrain. The MO Similarity Theory has been tested for wind and temperature profiles over fairly uniform and homogeneous terrains. We can also apply the MO Similarity Theory in our parameterization when multi-level, high frequency (>10 Hz) observations of wind and temperature are available.

The original MO Similarity Theory stated that the wind and temperature profiles are determined by several scaling parameters, u_*, T_*, and $\frac{z}{L}$, which are defined as follows:

$$u_* = [-\overline{(u'w')}_0]^{1/2} \tag{1}$$

$$T_* = -\overline{(w'\theta')}_0 / u_* \tag{2}$$

$$\frac{z}{L} = \frac{kzgT_*}{\theta_0 {u_*}^2} \tag{3}$$

where the superscript prime represents the turbulent fluctuation; over-bar denotes the averaged turbulence flux; subscript 0 denotes the fluxes are from the surface; k is the von Karman constant; z is the height; θ is the potential temperature; and L is the MO length. The ratio z/L is the surface layer atmospheric stability parameter. The resulting similarity profiles are (*7, 8*):

$$\phi_m(z/L) = (kz/u_*)(\partial u/\partial z) \tag{4}$$

$$\phi_h(z/L) = (kz/T_*)(\partial \theta/\partial z) \tag{5}$$

where ϕ_m and ϕ_h are the non-dimensional momentum and heat functions. These formulations are given in Businger *et al*. and Dyer (*7, 9*).

The u_*, T_*, and *z/L* are calculated using equation 1 to 3. The non-dimensional momentum and temperature functions can be computed using following formulations derived from many observations (*9, 10*):

$$\phi_m = (1+16\,|\,z/L\,|)^{-1/4} \quad \text{for } -2 \le z/L \le 0, \quad \text{unstable condition}$$

$$\phi_m = (1+5z/L) \quad \text{for } 0 \le z/L \le 1, \quad \text{stable condition} \tag{6}$$

$$\phi_h = (1+16\,|\,z/L\,|)^{-1/2} \quad \text{for } -2 \le z/L \le 0, \quad \text{unstable condition}$$

$$\phi_h = (1+5z/L) \quad \text{for } 0 \le z/L \le 1, \quad \text{stable condition} \tag{7}$$

The wind and temperature profiles can be integrated using equation 4 and 5. The observational test of the MO Similarity Theory can be found in the literature (*7–10*).

3.2 Moderate Data Scenario: Multi-level Average Wind and Temperature

As seen in equation 1 and 2, the flux calculations that use fast response turbulence sensors are required to determine the momentum and heat fluxes. In the cases of fast response fluxes, when observations are not available, as in Project WIND, we propose using mean wind and temperature observations to parameterize the scaling parameters. This will ensure the slow

response wind and temperature sensor can be used for the similarity wind and temperature profiles. The key parameter for the surface layer atmospheric stability condition is described by the gradient Richardson number, R_i, which can be computed from the wind and temperature measurement at two heights:

$$R_i = \frac{g(\partial\overline{\theta}/\partial z)}{\overline{\theta}(\partial\overline{u}/\partial z)^2}. \quad (8)$$

Close to the ground surface (<10 m above ground), the R_i can be approximated with the bulk Richardson number, R_{ib},

$$R_{ib} = \frac{g}{\overline{\theta}} \frac{(\theta_2 - \theta_1)/(z_2 - z_1)}{(u_2 - u_1)^2} \quad (9)$$

where subscript 1 and 2 represent the time averaged variables from the surface and a higher point. When equations 4 and 5 are integrated, the following logarithmic profiles, modified by stability functions, are derived (*11*):

$$u(z) = \frac{u_*}{k}[\ln(z/z_0) - \psi_m] \quad (10)$$

$$T(z) = \frac{T_*}{k}[\ln(z/z_0) - \psi_h] \quad (11)$$

where the ψ_m and ψ_h are the integrals of $(1-\phi_m)/(z/L)$ and $(1-\phi_h)/(z/L)$, respectively, the z_0 is the roughness length, at which *u(z)* vanishes. Although it is strictly a flow property parameter (*12, 31*), the z_0 is parameterized as related to vegetation canopy height *h* in practice, i.e., z_0=0.075 *h to* 0.14 *h* (*31*). The z_0 can be approximately parameterized according to the land-use categories shown in table 2 (*13*), when the canopy height data is not available. The turbulence fluxes parameters, u_* and T_* can be computed from equation 10 and 11 using the observed mean value of *u* and *T* and parameterized ψ_m and ψ_h. The ψ_m and ψ_h are parameterized in the following sections, in different atmospheric stability conditions, using the Richardson number.

Table 2. Land use categories and roughness length.

3DWF Land Use Category (Same as MM5 Category)		USGS Land Use Category		Average Roughness Length (cm) Summer/Winter	
1	Agriculture land	2	Dry cropland and pasture	15	5
		3	Irrigated cropland and pasture		
		4	Mixed dryland/irrigated pasture		
2	Range-grassland	7	Grassland	12	10
		8	Shrubland		
		9	Mixed shrub/grassland		
		10	chaparral		
3	Deciduous forest	12	Broadleaf deciduous forest	50	50
		16	Deciduous coniferous forest		
4	Coniferous forest	13	Evergreen coniferous forest	50	50
		14	Sub alpine forest		
5	Mixed forest/wetland	6	Woodland/cropland mosaic	40	40
		15	Mixed forest		
6	Water	18	Water	.001	.001
7	Marsh or wetland	19	Herbaceous	20	20
		20	Forested wetlands		
8	Desert	21	Barren or sparsely vegetated	10	10
9	Tundra	22	Shrub and brush tundra	10	10
		23	Herbaceous tundra		
		24	Bare ground tundra		
		25	Wet tundra		
		26	Mixed tundra		
10	Permanent ice	27	Perennial snowfields or glaciers	5	5
11	Tropical forest	17	Evergreen broadleaf	50	50
12	Savannah	11	Savannah	15	15

3.2.1 Unstable Surface Layer

When R_{ib} <0, the surface layer is unstable. A relationship between the z/L and R_{ib} can be expressed as (*11*):

$$\frac{z}{L} \approx z/(z-z_0)\ln(z/z_0)R_{ib}\,. \tag{12}$$

The functions ψ_m and ψ_h for unstable condition have the following form (*14*) by the integration of equations 4 and 5:

$$\psi_m = 2\ln[(1+x)/(1+x_0)] + \ln[(1+x^2)/(1+x_0{}^2)] - 2\tan^{-1}(x) + 2\tan^{-1}(x_0) \quad (13)$$

and

$$\psi_h = 2\ln[(1+y)/(1+y_0)] \quad (14)$$

where

$$x = [1-15(z/L)]^{1/4}, \quad x_0 = [1-15(z_0/L)]^{1/4}, \quad y = [1-9(z/L)]^{1/2},$$

and

$$y_0 = [1-9(z_0/L)]^{1/2}.$$

By combining equations 10, 11, 12, 13, and 14, one can solve the turbulent scaling parameters, the mean wind, and the temperature profiles in an unstable condition. A lookup table for the values of ψ_m as a function of *z/L* is used to reduce computation time (*15*).

In the scenario of mean wind and temperature observation, figure 2 shows the MO similarity approach. The observed data is from OT1 in the open field during Project WIND (data set on JD 269). The wind profiles were averages from each 10-min time series. The wind direction was persistently flowing to the edge at 320° NW. In this case, the MO similarity approach simulated the mean wind profile very well. There is an underestimation of approximately 5% wind speed in the lower part of the wind profile, compared to the observed value. It is not surprising that the MO Similarity Theory worked well for this particular case, since the site is located in a very uniform flat terrain, and the wind was strong and nearly steady. The local equilibrium of turbulence production and dissipation was well-satisfied. However, the wind observed at the edge of OT2 does not satisfy the equilibrium assumption and the profile is different from OT1. The parameterization and discussion of forest edge wind will be deferred to section 4 of this document.

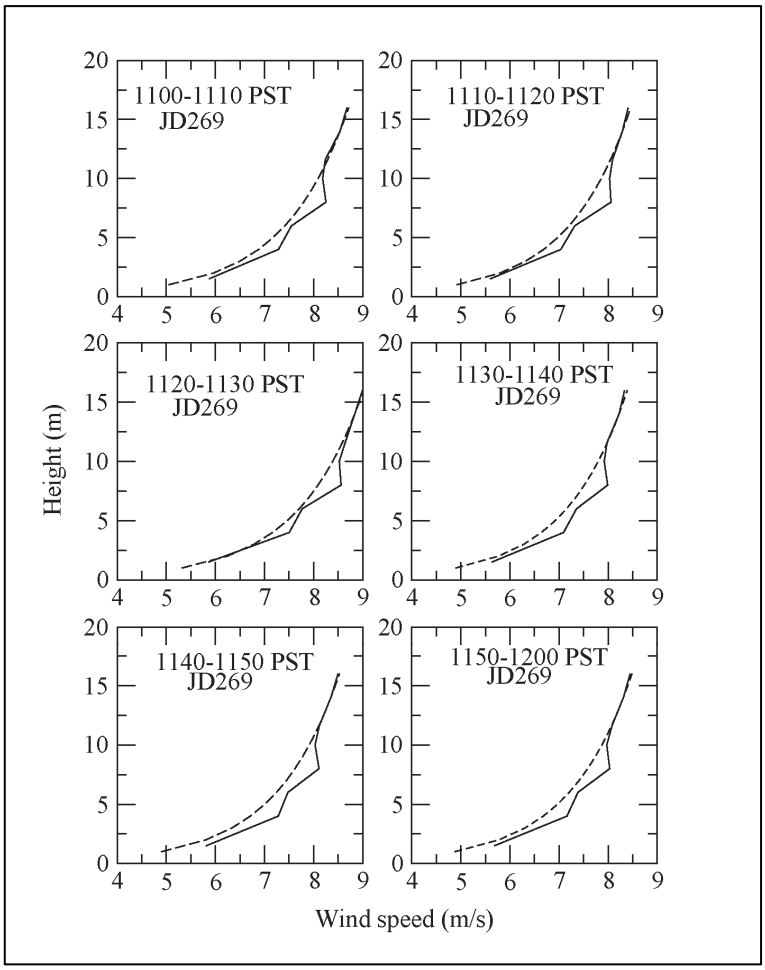

Figure 2. Wind profiles in strong wind and unstable atmospheric boundary layer stability conditions. Solid line represents horizontal wind at OT1. Dashed line represents the parameterization fit using the MO Similarity Theory.

3.2.2 Neutral Surface Layer

When the bulk Richardson number R_{ib} is very near 0 ($|R_{ib}| < 0.01$), the ψ_m is equal to zero. The resulting wind and temperature is a logarithmic profile:

$$u(z) = \frac{u_*}{k}[\ln(z / z_0)] \tag{15}$$

$$T(z) = \frac{T_*}{k}[\ln(z / z_0)]. \tag{16}$$

Figure 3 shows the similarity result for wind profiles in the neutral condition. The neutral atmospheric boundary layer appeared in transition time periods from either unstable to stable (evening, top two panels) or stable to unstable (morning, bottom two panels). We found that

both transition periods were short, usually from 20 to 30 min. The MO Similarity Theory was moderately successful for these neutral cases since the wind was weak and unsteady.

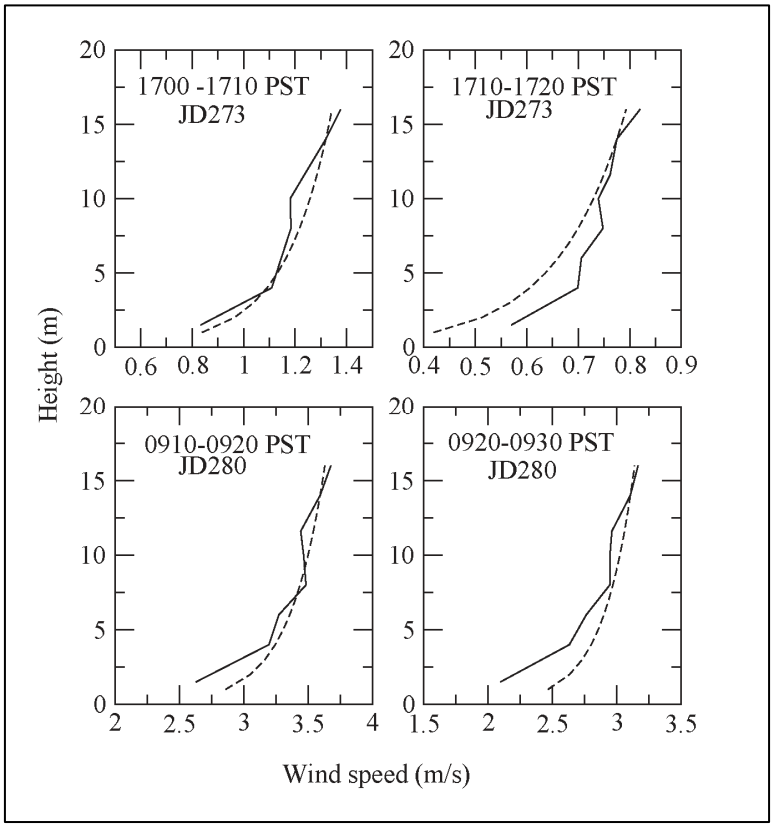

Figure 3. Wind profiles in weak to moderate wind speed and neutral atmospheric boundary layer stability condition. Solid line represents horizontal wind at OT1 and dashed line represents the parameterization fit using the MO Similarity Theory.

3.2.3 Stable Surface Layer

For weak stable boundary layers, the similarity parameterization has a very limited success. For moderate and strong stable atmospheric boundary layers, the MO Similarity Theory is not well-established for three reasons. First, the stable boundary layer is usually very shallow and difficult to observe. Second, the stable boundary layer is often associated with the intermittent turbulence, which is difficult to characterize. Third, the turbulence is not only produced by the surface friction, but is also advected from the low-level jet or wave breaking (*16*). The MO Similarity Theory is based on the local balance of turbulence production and dissipation; therefore, we would not expect it to describe the moderate to very stable boundary layer. Although general conclusions are not available, the stable boundary layer has been a very intensive research area in boundary layer meteorology. We will use the observed mean wind profile as the basis to initialize the model. The forest edge and interior canopy wind profiles are extrapolated empirically from the observed open field profile.

In figure 4, a time series of wind profiles in the stable condition are shown where the wind speed at OT1 had almost a linear increase with the height. Wind profiles at OT2 and OT3 show similar values since the wind direction flowed out of the edge at 150° SE. The near linear profile in open terrain was probably related to the nocturnal low-level jet (LLJ). From data sets, CASEX 99 (*17*) and JU2003 (*18, 19*), we know the nocturnal LLJ is common a phenomena in the clear, undisturbed night atmosphere. The data showed the nocturnal LLJ was observed in 9 out of 10 intensive observation periods (*18*). A linear profile file would be a fit for this condition, because the surface layer is very shallow and the linear trend wind profile is a distinct character of the very stable boundary layer due to the LLJ. Figure 4 shows that the wind profiles are nearly linear above 2.5 m for open field tower OT1. The wind profiles for OT2 and OT3 will be discussed in later sections.

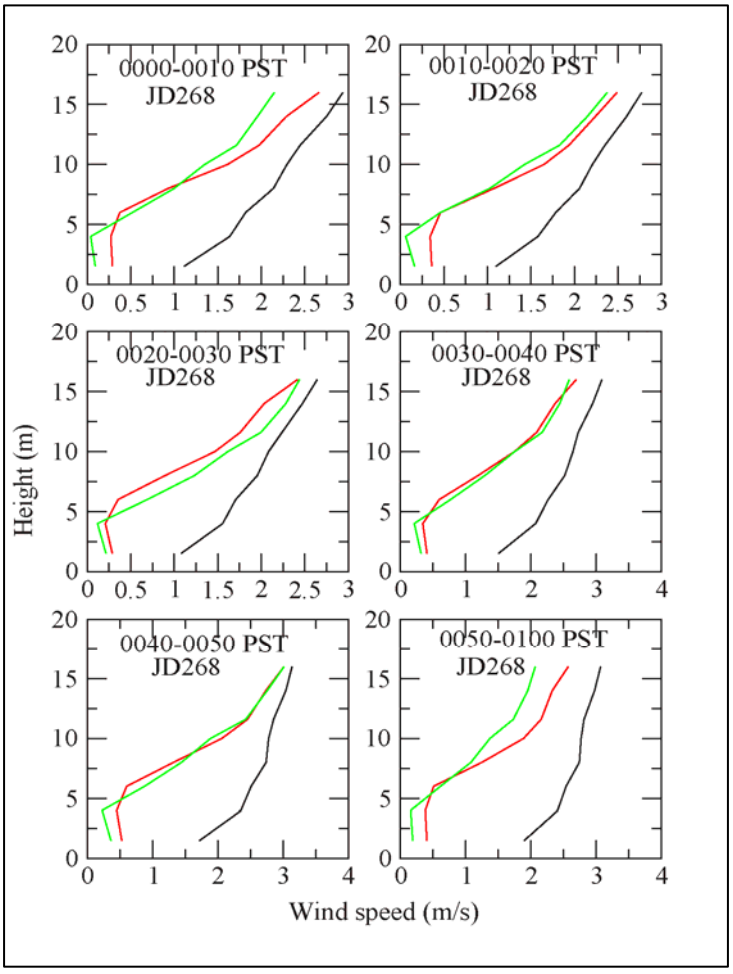

Figure 4. Wind profiles during a stable atmospheric condition. OT1 is represented with a black line, OT2 a red line, and OT3 a green line. Air was flowing out of the orchard edge.

3.3 Data Poor Scenario: Only One Point Observation is Available

Under the data scarce condition, the following power law profile will be used (*3*):

$$u(z) = u_m (z / z_m)^P \tag{17}$$

where z is the height above the ground, u_m is the one point measured wind speed, z_m is the measurement height, and the superscript P is the power coefficient which determines the rate of increase of wind speed with height. Peterson and Hennessey (*4*) have assigned a value of P of 0.143 for neutral flow over land and P of 0.286 over water. However, our analysis indicated that the exponential value P = 0.17 to 0.20 fit the portion of data in an unstable case better than those previously suggested. Figure 5 shows how the exponential profile fits to the OT1 data for the unstable case during JD269. The exponential profile overestimated the wind speed at the upper portion of the profile. As expected, the accuracy of exponential fit was not as good as the MO similarity approach. Therefore, when multi-level wind and temperature observations are not available, this approach is the only viable choice.

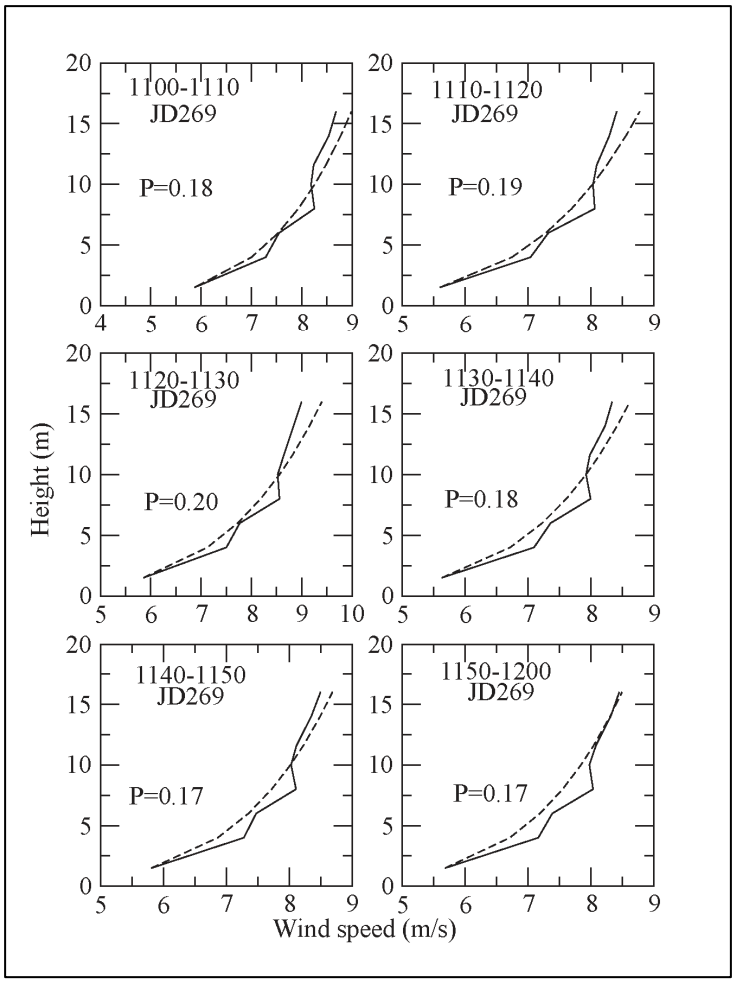

Figure 5. Exponential fits (dashed line) of wind profiles at OT1 using different *P* values.

4. Wind Profile Within and Above Vegetation Canopies

4.1 Mean Flow Within Plant Canopy

The vegetation canopy is considered the roughness sublayer (RSL). Mean wind speed is reduced in the plant canopy due to the form and friction drags of leaves, stalks, and branches. A large portion of the mean kinetic energy is converted to turbulent kinetic energy by the canopy elements. The turbulence intensities are much higher than those found in the surface layer of uniform terrain without vegetations. The mean wind shear reaches its maximum value at the top of the canopy. An exponential wind profile model has been proposed (*20, 21, 33, 34*) for the mean wind in plant canopies as:

$$u(z) = u_h \exp[\alpha(z/h - 1)] \tag{18}$$

where h is the average plant canopy height, u_h is the mean wind at the canopy height, and α is the canopy flow index. This model has been validated in various observational studies in homogeneous plant canopies (*22–26*). The canopy flow index, α, is related to the leaf area density and canopy element geometrical characteristics. Cionco (*26*) has given a list of canopy flow index values for different plant canopies. He indicated α is also related to the canopy element flexibility and wind speed. Additionally, Kaimal and Finnigan (*15*) list a number of canopy flow indexes from other observational studies. Table 3 shows a survey of available canopy flow index values from various studies, and the trend that α value is inclined to increase with the leaf area index (LAI). Note that LAI values are not always reported along with the meteorological data.

Table 3. Average canopy flow index reported from the literature.

Canopy	Leaf Area Index (LAI)	Canopy Flow Index, α
Corn (Shaw *et al*., 1974)	3.0	2.4
Corn (Wilson *et al*., 1982)	2.9	4.1
Forest (Raupach *et al*., 1996)	1.0	1.7
Wheat (Cionco, 1978)		2.5
Gum-maple (Cionco, 1978)		4.42 ± 1.05
Maple-fir (Cionco, 1978)		4.03 ± 0.69
Jungle (Cionco, 1978)		3.84 ± 1.52
Spruce (Cionco, 1978)		2.74 ± 1.29
Oak-gum (Cionco, 1978)		2.68 ± 0.66

4.2 Mean Flow Above Plant Canopy

The logarithmic profile is valid over a homogeneous plant canopy; however, the origin of the profile has moved to a level at height *d,* which has been named the displacement height. The exact value of the displacement height is dependent of canopy leaf density and structures. A commonly use value is $0.5 – 0.75h$ (*15, 26*), where h is the average canopy height. Using the displacement height, the non-dimensional similarity profiles above the canopy become:

$$\phi_m(z/L) = [k(z-d)/u_*]\partial u/\partial z \tag{19}$$

$$\phi_h(z/L) = [k(z-d)/T_*](\partial\theta/\partial z)\,. \tag{20}$$

Equations 19 and 20 can be also integrated for the wind and temperature profiles in and above the plant canopy. However, the roughness lengths for momentum and other scalars are different (*27*). The roughness length for the wind profile represents the capacity of the canopy to absorb the momentum, while the roughness length for the temperature profile express the capacity of the canopy to absorb (or emit) the heat or other scalars such as CO_2 (*15*). The canopy is far more efficient at absorbing momentum than at absorbing the scalars, which is called the "bluff body effect". This is because the momentum is primarily transported to the canopy element by pressure drag, which is nonexistent in a scalar transport. Hence, the roughness length for scalar is about one-fifth of the value for the momentum (*15*). As we discussed in section 3, the roughness length is a flow property parameter (*13, 31*) and changes with flow and roughness

conditions. The z_0 is parameterized as related to vegetation canopy height h in practice, i.e., z_0=0.075 h *to* 0.14 h (*31*). For our modeling purpose, momentum roughness length is z_0 = 0.05h. Table 2 lists the roughness length values for different land use categories in case the canopy height data is not available.

The wind profile from OT3 in the orchard canopy plotted in figure 6 is very different from OT1 in open terrain. A large reduction in wind speed is shown between the towers. For the strong wind and unstable condition shown in figure 6, the combined subcanopy and above canopy flow using equations 18, 19, and 20 give a fairly good prediction compared with the data at the OT3 location. Generally, the similarity profiles underestimated the wind speed at subcanopy (<4m) and above canopy (>10m).

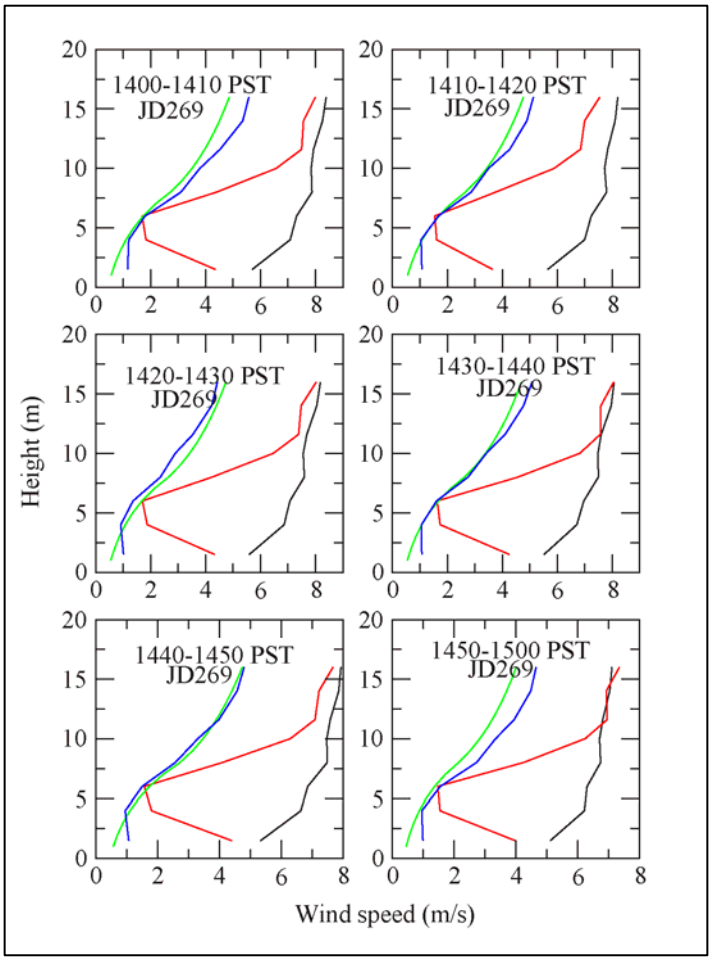

Figure 6. Horizontal wind profiles during strong unstable wind conditions when flowing into the orchard. OT1 black lines, OT2 red lines, OT3 blue lines, and the green lines are the parameterized wind profiles for the interior OT3 location.

Figure 7 shows that for the weaker wind and near neutral condition, the similarity theory above the canopy performed less satisfactory than in the strong wind case (section 5). Multiple tests

with Project WIND data indicated that α=1.8, u_*=1.2 u_{*o}~1.5u_{*o} (open field), z_0=0.4m, and d=4m give the best wind profile parameterization.

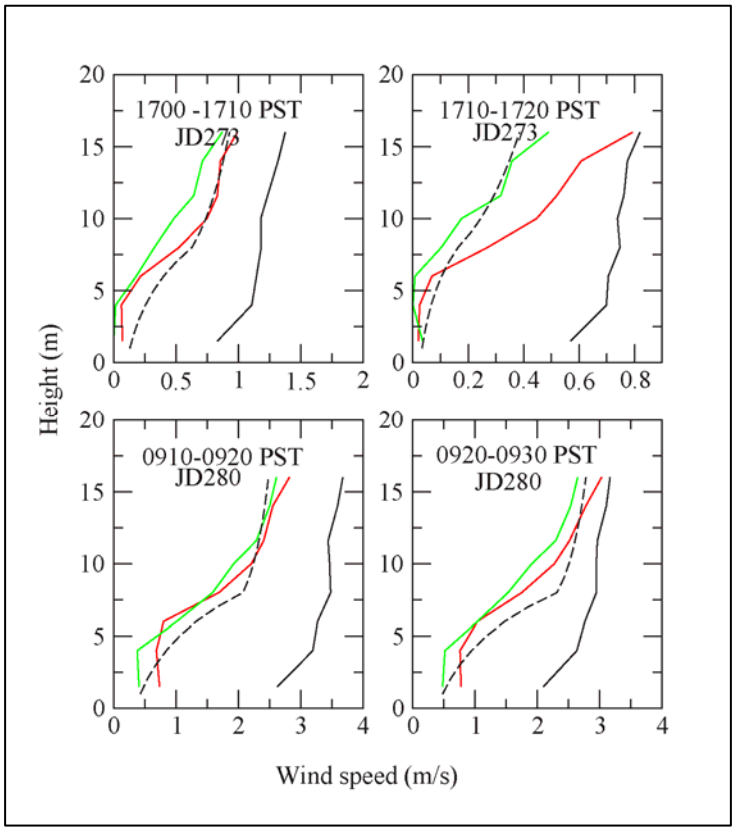

Figure 7. Horizontal wind profiles for weak and neutral wind conditions. OT1 black lines, OT2 red lines, OT3 green lines. The dashed lines are the parameterized wind profiles for the interior OT3 location.

It is important to emphasize that parameters z_0 and d are also flow parameters (*28*). The parameters given in table 3 are only dependent of the land use category and are merely rough estimates of z_0. The values may change with different wind conditions. An improvement of the wind above the uniform forest canopy has been reported recently by Harman and Finnigan (*29*). The model views the above canopy flow as the RSL originally proposed by Raupach *et al*. (*30*). In this theory, the RSL has a high vorticity generated by the shear. The Kelvin-Helmholtz instability dominated this layer. Harman and Finnigan's (*29*) initial results also indicated that the standard MO Similarity Theory usually underestimated the wind speed above the canopy. We will investigate the new RSL approach further in our future studies.

Although using the MO Similarity Theory in the wind profile at the above vegetation canopy is valid for the uniform canopy, a great deal remains unknown for the non-uniform canopy. We propose the parameterization scheme that follows for the non-uniform canopy. Given the nearby open field wind profile, the wind profile above the canopy level is around 40% of the wind speed at the same height in the open field. The canopy momentum absorption is gradually reduced

from the canopy height to about the 3-canopy height level. The slow-down factor is linearly decreased from 60% at the canopy level to 0% at the 3-canopy height level. The proposed scheme is based on the wind profiles in the orchard observation shown in figures 4 and 6. This parameterization scheme will be tested with other observation data sets when they are available.

4.3 Mean Wind in the Transition Regions at Forest Edge

The wind in the transition region of the forest edge is more complex than the flow in an interior homogeneous forest without the edge effect. Near the edge region, atmospheric flow experiences an abrupt change in roughness and turbulence production and dissipation is not locally balanced; therefore, the standard MO Similarity Theory is not expected to apply. Another complexity is that the flow is extremely dependent on wind directions. Wind that blows into the forest edge behaves quite differently from the wind that blows out of the forest edge. The wind that is perpendicular to and not perpendicular to the forest edge is also different.

The orchard data from Project WIND shown in figure 6 indicate the wind profiles at the edge deviate greatly from the other towers. When the air was flowing into the forest edge, the wind profile at the canopy region experienced the same slow down as OT3; however, the shear was stronger above the canopy compared to OT3. The wind speed was almost equal to the speed at the same height of the interior tower in the crown region (3–8 m), and nearly reached the 95% wind speed of OT1 at 12 m (1.5 times canopy height). The wind speed in the trunk space was greater than in the interior orchard, due to the absence of other vegetative growth. In a natural forest edge, vegetative growth often fills the trunk space and the profile is probably different from the orchard case.

The wind profile at the edge can be parameterized by piecewise linear interpolation according to the observed data from figures 4, 6, and 7. The basic idea of wind flow parameterization into and out of the forest canopy is illustrated in figure 8. The inflow region affected by the forest edge is assumed to be 2–3h; this is where the flow is interpolated linearly from the open to the edge flow profile within the 2h region. The flow transition from the edge to the fully developed canopy flow area is taken as 5–10h. The outflow region affected by the canopy edge is about 4–6h. The distances for the flow adjustment are related to the canopy density, with longer distance for the sparse canopy and shorter distance for the dense canopy (*32*).

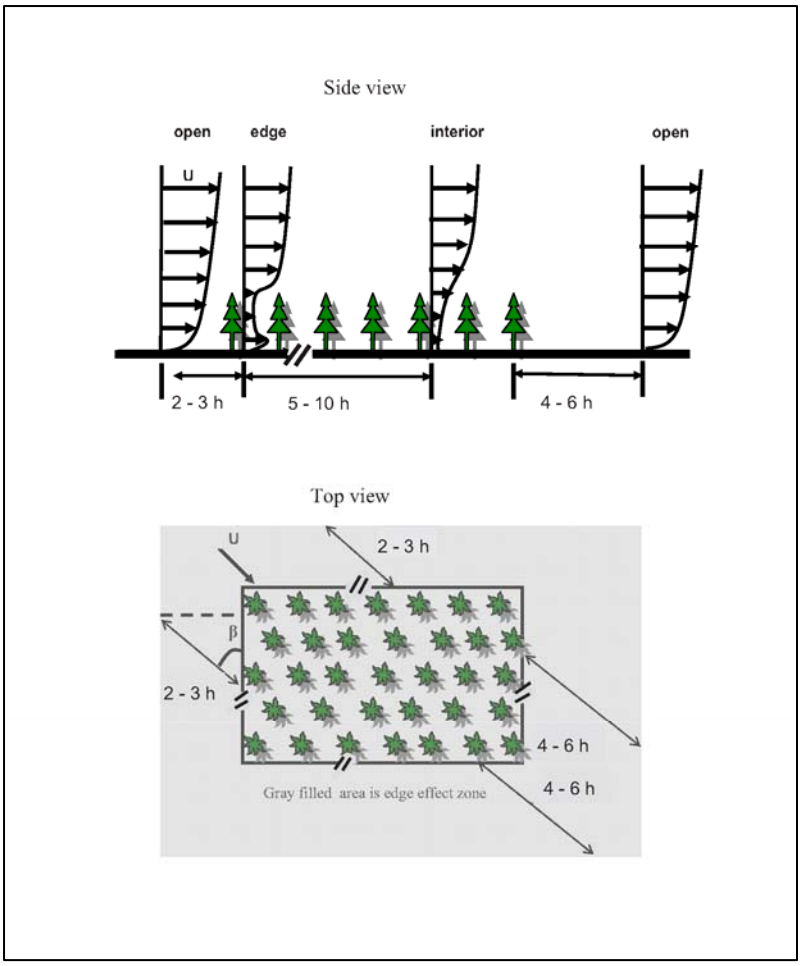

Figure 8. Schematic diagram to demonstrate wind profile parameterization in the leading and trailing edge of forest. It takes 2–3*h* to adjust to the edge wind profile in the leading edge; 5–10*h* to reach the interior equilibrium profile; and 4–6*h* to adjust to the open field wind profile. The shaded area is affected by the forest and forest edges.

The wind profiles above canopy and in the crown region are set to equal the interior region without the edge effect. The profile in the trunk space and above 1.5*h* is set the same as OT1. The wind profile at the OT2 is parameterized as follows for wind flowing into the edge:

$$u_e(z) = \frac{z-h}{0.5h}\left[(0.95u_{0(1.5h)} - u_{f(h)}\right] + u_{f(h)} \qquad \text{for} \qquad h \le z \le 1.5h \quad \text{(above canopy)}$$

$$u_e(z) = u_{f(h)} \quad \text{for} \quad 0.5h < z < h \quad \text{(in the crown region)} \tag{21}$$

$$u_e(z) = u_0(z) \qquad \text{for} \qquad 0 \le z \le 0.5h \ \text{ and } \ z \ge 1.5h \ \text{ (above } 1.5h\text{)}$$

where subscripts *o, f,* and *e* stand for open field, forested region, and forest edge, respectively, and represent the wind values at the OT1, OT3, and OT2. The wind speed in the open terrain at 1.5 times canopy height is $u_{0(1.5h)}$, the wind speed at canopy height in the orchard is $u_{f(h)}$, and

the wind speed at the edge tower location is $u_e(z)$. The wind profiles above the canopy and in the trunk space is parameterized to change gradually from the edge to about *3h* distance inside the orchard, where *h* is the canopy height. The variation is parameterized by interpolating the edge and interior tower profiles linearly.

The change in the wind profiles at the edge and interior of the orchard was insignificant when the wind was from the orchard edge as shown in figures 4 and 7. Therefore, the wind profile parameterized for OT3 inside the orchard when the wind blows out the orchard edge. The wind profiles between OT2 and OT1 made a gradual adjustment using a linear interpolation.

5. Application of Wind Profile Parameterizations in the 3DWF and Comparison with Project WIND Data

The objective of this analysis is to create a scheme to parameterize the mean wind in a gentle terrain and forest canopy (including the edge regions) when limited observation data is available. Project WIND has collected a large amount data that is useful to validate this scheme. In the validation procedure, the wind profile in OT1 is used as the only input, which is the usual scenario because the observation in an open field is much easier than that in a forest. The wind profiles in the edge transition areas and the interior of the forest are parameterized. After running the 3DWF, a three-dimensional mass-consistent diagnostic wind field is generated. The computed wind field is then compared with the available wind observations at the locations and heights of OT2 and OT3. Two sets of data were selected for this purpose. The first case (data set JD269) was in a daytime: the wind is strong, the thermal condition was slightly unstable, and air was flowing into the orchard edge. The second case (data set JD268) was during a night: the wind speed was moderate, temperature was in strong stable thermal stratification, and the wind direction was flowing out from the orchard edge.

5.1 Validation with the Strong Wind Case

Figure 9 shows a sample of simulation results (1410 UTC, JD269) when a strong wind is flowing into the orchard edge. The thermal condition is slightly unstable with gradient *Ri* of -0.12. The top panel shows a vertical y-z slice cutting through the center of the computational domain at x=320 m. The white sticks represent the three observation towers during Project WIND. The wind in and above the orchard canopy show different wind distributions compared to the wind in the open field. The wind in the canopy was about 15% of open field in magnitude in the trunk space, and 25% of open field in the crown region. Above the canopy the wind speed was lower than the open region at same height. The wind gradually increased with the height and eventually reached the same magnitude at the 3*h* (24 m) height. There was a redevelopment of the internal boundary layer according to the higher roughness of the canopy at the leading edge of the orchard. Since the wind was flowing into the edge trunk open area, the wind in the trunk

region had local maxima. The bottom panel of the plot shows the wind speed and direction at 2 m height. The wind speed in the transition region started at the 2*h* from the edge (at y=350 m) and gradually decreased to an equilibrium value at y=275 m (about 5*h* from the edge).

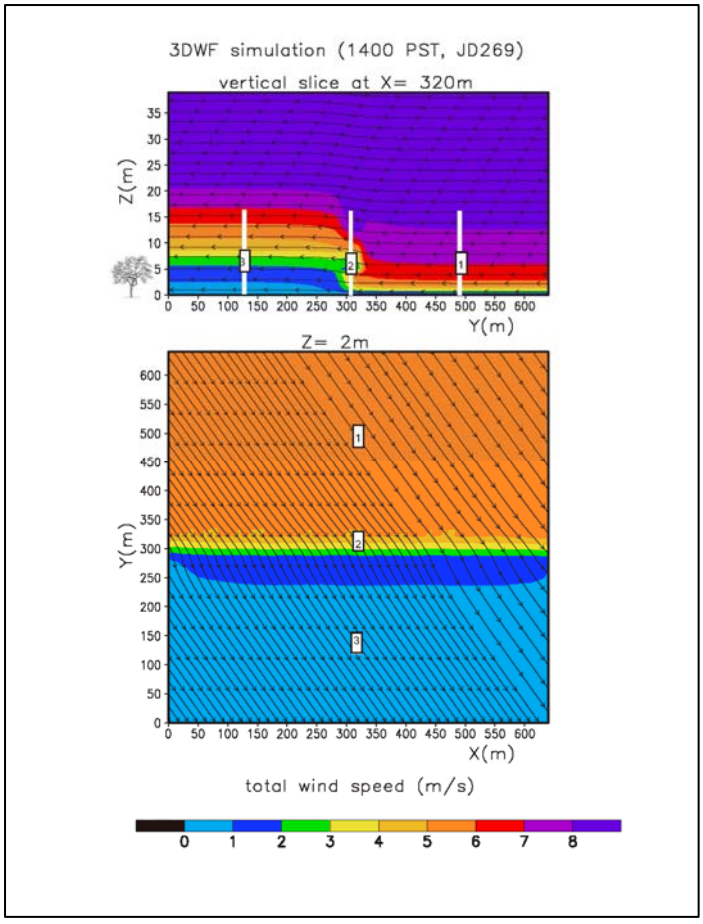

Figure 9. A sample of 3DWF simulation results using the OT1 data as input with unstable strong wind conditions. Air was flowing into the orchard edge. The top panel is the vertical cross section at X = 320 m, and the bottom panel is the horizontal cross section at Z = 2 m.

A statistics of error for the simulation during a one-hour period with 10-min sections can be computed at OT2 and OT3. The relative root-mean-square (*rms)* error for horizontal winds can be defined as:

$$rms = \left[\frac{\sum_{n=1}^{N} (u_m - u_b)_n^2 + \sum_{n=1}^{N} (v_m - v_b)_n^2}{\sum_{n=1}^{N} (u_b)_n^2 + \sum_{n=1}^{N} (v_b)_n^2} \right]^{1/2}$$

where N is the total number of observation points for a tower, subscript b represents the observational values, and subscript m represents the model simulation value. The *rms* represents the average error percentage compared with the observation. Table 4 lists the averaged *rms* values from the location of orchard edge and inside orchard. The *rms* value indicates the prediction skill for 3DWF captured 75% to 81% of flow field. The predicted value at the interior of the orchard agreed more with the observation than at the orchard edge for the flow into edge case. The difference, between the observed and simulated values, showed a larger value in the interior of forest than for the stable flow out from the orchard edge case.

Table 4. Averaged relative rms values for horizontal wind simulation.

Time and Data Set Number	Wind Relative to the Orchard	Stability Condition	OT2 rms at Edge	OT3 rms in Orchard
1400-1500 PST, JD269	Flow into the edge	Unstable	0.22	0.19
0000-0100 PST, JD268	Flow out from edge	Stable	0.20	0.25

5.2 Validation with Moderate Wind, Stable Condition

Figure 10 shows a sample of simulation results (0010 UTC, JD268) when a moderate wind is flowing out from the orchard edge. The thermal condition was stable with gradient *Ri* of 0.27. The top panel shows a vertical y-z slice cutting through the center of the computational domain at x=320 m. The white sticks represent the three observation towers used during Project WIND (OT1, OT2, and OT3). The wind in and above the orchard canopy show different wind distributions compared to the open field. The wind speed was lower above canopy, than in the open region at the same height. The wind gradually increased with the height and reached the same magnitude at the 3h (24 m) height. Compared to the wind flowing into the edge case, the wind profiles at OT2 and OT3 were similar. The boundary layer began its adjustment to the smoother open field surface at the trailing edge of the orchard and reached equilibrium at 355 m (about 4h from edge). The bottom panel in figure 10 shows the wind speed and direction at 2 m height. Except in the edge transition area, the wind field is basically uniform. The *rms* value indicated the prediction skill for 3DWF captured approximately 75% of the flow field. The lower prediction skill probably reflects the thermal stratification in weaker wind condition has a significant impact on the flow field.

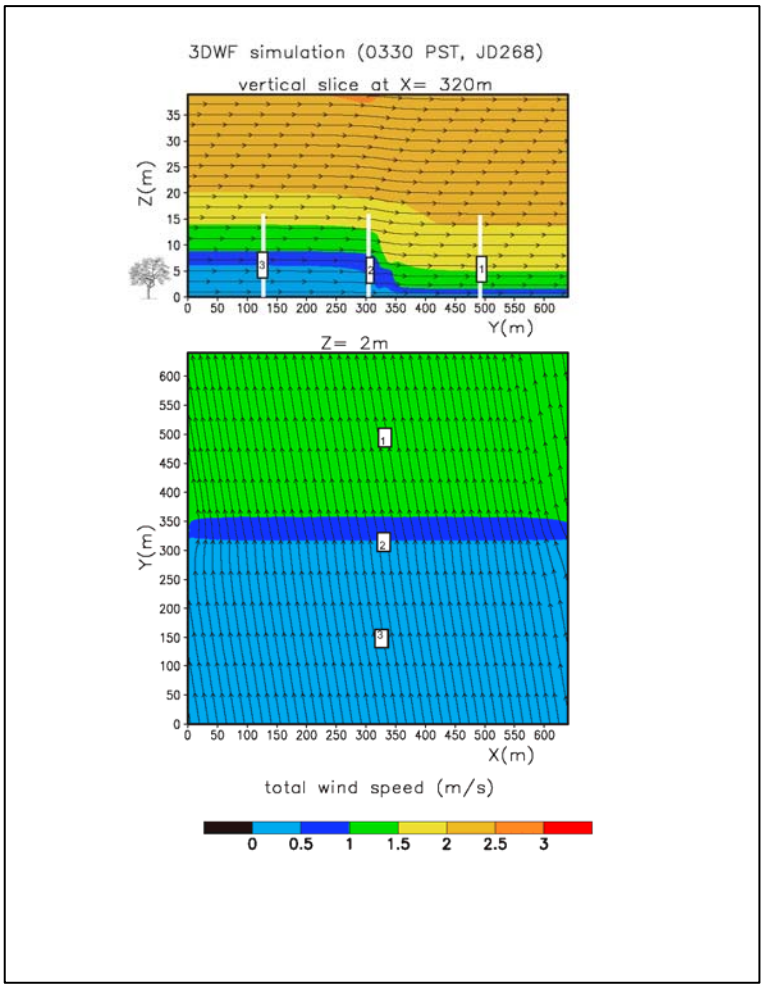

Figure 10. A sample of 3DWF simulation results using the OT1 data as input with stable, moderate wind conditions. Air was flowing out of the orchard edge. Top panel is the vertical cross section at X = 320 m, and the bottom panel is the horizontal cross section at Z = 2 m.

Figure 11 shows a sample result of 3DWF simulation for a strong wind condition in 3D. The wind directions and magnitude are represented by the red cones. The wind profiles in the edge transition and interior orchard are parameterized using the parameterization scheme discussed in sections 4 and 5. After the mass-consistent adjustment, a 3D wind field is computed. The figure compares the wind vectors at the exact same locations at the tower observation.

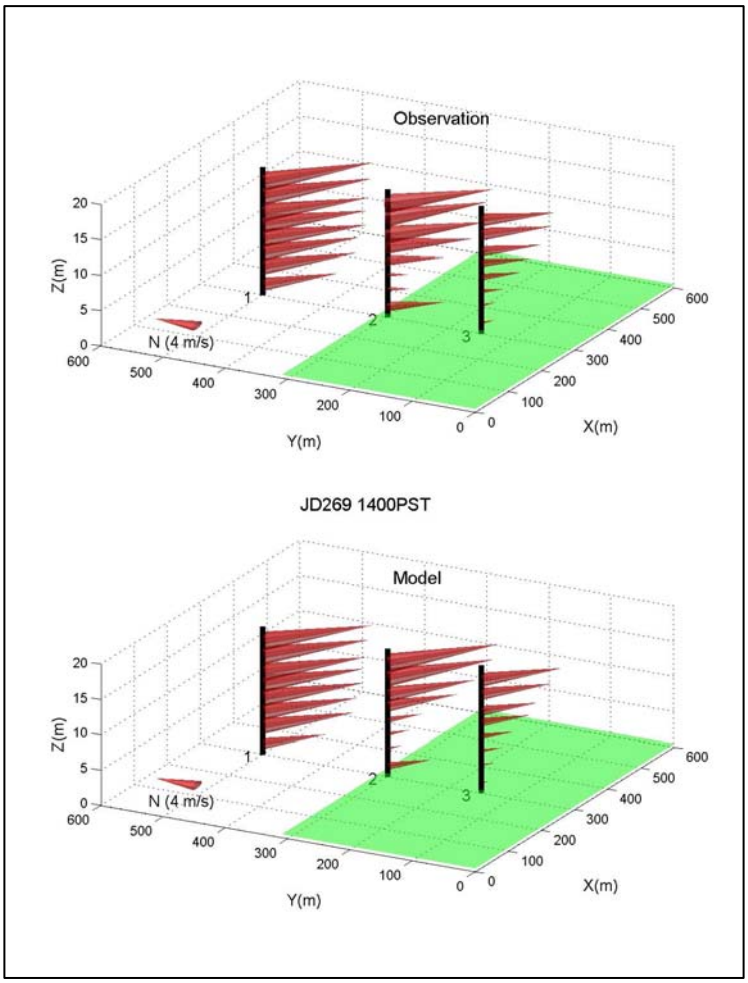

Figure 11. A 3D plot of a 3DWF simulation (lower panel) compared the observation (upper panel). The green areas denote the orchard area.

6. Summary and Conclusion

A wind profile parameterization scheme for a gentle slope with and without vegetation is proposed. For an open field, the proposed scheme considered several data source scenarios: rich data, moderate data, and poor data availability. Under the data rich scenarios, such as multiple tower and level observations or systematic Doppler lidar scans, the observed wind profiles can be directly applied for model initialization. In moderate data source scenarios, such as multi-level instruments on a single tower, a bulk Richardson number based on stability categories can be classified. The MO Similarity Theory can be applied to this situation. The similarity parameters, such as the displacement height and roughness length, need more observational data or literature to better represent them. In a data poor scenario, such as the single point observation, a power-law profile can be used with less accuracy compared to the MO Similarity

Theory. A simple similarity profile above the canopy and an exponential profile in canopy are used for a wind profile in a vegetation canopy. Because of the limited amount of data from Project WIND, the treatment of the plant canopy edge effect on the wind profile is also proposed.

The proposed parameterization has been partially tested with Project WIND data. The limited evaluations indicate that the 3DWF model using this initialization scheme captured the basic feature of the wind field. This study only touches a simple condition of gentle terrain covered with a uniform forest canopy. Further studies are needed to evaluate complex situations such as terrain with steeper slopes and non-uniform forest canopies.

References

1. Wang, Y.; Mercurio, J. J.; Williamson, C. C.; Garvey, D. M.; Chang, S. *A High Resolution, Three-Dimensional, Computationally Efficient, Diagnostic Wind Model: Initial Development Report*; ARL-TR-3094; U.S. Army Research Laboratory: Adelphi, MD, 2004.

2. Wang, Y.; Williamson, C.; Garvey, D.; Chang, S.; Cogan, J. Application of a Multigrid Method to a Mass Consistent Diagnostic Wind Model. *J. Appl. Meteorol.* **2005**, *44*, 1078–1089.

3. Hanna, S. R.; Briggs, G. A.; Hosker, R. P. Handbook on Atmospheric Diffusion, DOE/TIC-11223, U.S. Dept. of Energy, Oak Ridge, TN, 1982.

4. Peterson, E. W.; Hennessey, J. P., Jr. On the Use of Power Laws for Estimates of Wind Power Potential. *J. Appl. Meteorol.* **1978**, *17*, 390–394.

5. Cionco, R. M. Design and Execution of Project WIND. *Proceedings of the 19th Conference on Agriculture and Forest Meteorology,* Charleston, SC, March 7–10, 1989, American Meteorology Society, Boston, 1989.

6. Monin, A. S.; Obukhov, A. M. Basic Laws of Turbulent Mixing in the Ground Layer of the Atmosphere. *Trans. Geophys. Inst. Akad. Nauk USSR* **1954**, *151*, 163–187.

7. Businger, J. A.; Wyngaard, J. C.; Izumi, Y.; Bradley, E. F. Flux-Profile Relationships in the Atmospheric Surface Layer. *J. Atmos. Sci.* **1971**, *28*, 181–189.

8. Haugen, D. A.; Kaimal, J. C.; Bradley, E. F. An Experimental Study of Reynolds Stress and Heat Flux in the Atmospheric Surface Layer. *Quart. J. Roy. Meteorol. Soc.* **1971**, *97*, 168–180.

9. Dyer, A. J. A review of flux-profile relationships. *Boundary-Layer Meteorol*. **1974**, *7*, 363–372.

10. Högstrom, U. Nondimensional wind and temperature profiles. *Boundary-Layer Meteorol.* **1988**, *42*, 55–78.

11. Panofsky, H. A.; Dutton, J. A. *Atmospheric Turbulence*; Wiley-Interscience: New York, NY, 1984; 397.

12. Grell, G. A.; Dudhia, J.; Stauffer, D. R. *A Description of the Fifth-Generation Penn State/NCAR Mesoscale Model (MM5)*; NCAR/TN-398+STR, NCAR Technical Note, 1994.

13. Finnigan, J. J. Turbulence in Waving Wheat. I. Mean Statistics and Honami. *Boundary-Layer Meteorol*. **1979**, *16*, 181–211.

14. Paulson, C. A. The Mathematical Representation of Wind Speed and Temperature Profiles in the Unstable Atmospheric Surface Layer. *J. Appl. Meteorol*. **1970**, *9*, 857.

15. Kaimal, J. C.; Finnigan, J. J. *Atmospheric Boundary Layer Flows*. Oxford Univ. Press: NY, 1994.

16. Mahrt, L. Stratified Atmospheric Boundary Layers. *Boundary-Layer Meteorol.* **1999**, *90*, 375–396.

17. Banta, R. M.; Newsom, R. K; Lundquist, J. K; Pichugina, Y. L; Coulter, R. L.; Mahrt, L. Nocturnal Low-Level Jet Characteristics over Kansas during CASES-99. *Boundary-Layer Meteorol.* **2002**, *105*, 221–252.

18. De Wekker, S.F.J.; Berg, L. K.; Allwine, J.; Doran, J. C.; Shaw, W. J. Boundary-layer structure Upwind and Downwind of Oklahoma City during the Joint Urban 2003 Field Study. *Proceedings of the 5th AMS Conference on Urban Environment,* Vancouver, B.C. Canada, August 23–27, 2004.

19. Wang, Y.; Klipp, C.; Garvey, D.; Ligon, D.; Williamson, C.; Chang, S.; Newsom, R.; Calhoun, R. Nocturnal Low-level jet Dominated Atmospheric Boundary Layer Observed by Doppler Lidars over Oklahoma City during June 2003. *J. Appl. Meteorol.* 2007 (in press).

20. Cionco, R. M. A mathematical model for air flow in the vegetative canopy. *J. Appl. Meteorol*. **1965**, *4*, 517–522.

21. Inoue, E. On the turbulent structure of airflow within crop canopies. *J. Meteorol. Soc. Japan* **1963**, 317–326.

22. Shaw, R. H.; Silversides, R. H.; Thurtell, G. W. Some Observations of Turbulence and Turbulent Transport Within and Above Plant Canopies. *Boundary-layer Meteorol*. **1974**, *5*, 429–449.

23. Shinn, J. H. Steady-State Two-Dimensional Flow in Forests and the Disturbance of Surface Layer Flow by a Forest Wall; R&D Technical Report ECOM-5583; Fort Monmouth, NJ; 1971.

24. Baldocchi, D. D.; Meyers, T. P. Turbulence Structure in a Deciduous Forest. *Boundary-Layer Meteorol*. **1988**, *43*, 345–364.

25. Amiro, B. D. Drag coefficients and turbulence spectra within three boreal forest canopies. *Boundary-Layer Meteorol*. **1990**, *52*, 227–246.

26. Cionco, R. M. Analysis of canopy index values for various canopy densities. *Boundary-Layer Meteorol*. **1978**, *15*, 81–93.

27. Thom, A. S. Momentum Absorption by Vegetation. *Quart. J. Roy. Meteorol. Soc.* **1971**, *97*, 414–428.

28. Finnigan, J. J. Turbulence in Waveing Wheat. I. Mean Statistics and Honami. *Boundary-Layer Meteorol.* **1979**, 181–211.

29. Harman, I. N.; Finnigan, J. J. The impact of a dense canopy on the wind profile and evolution of a boundary layer. *Proceedings of Amer. Meteorol. Soc. 26th Boundary Layer and Turbulence. San Diego, CA,* May 2006.

30. Raupach, M. R.; Finnigan, J. J.; Brunet, Y. Coherent Eddies in Vegetation Canopies: The Mixing Layer Analogy. *Boundary-Layer Meteorol.* **1996**, *78*, 351–382.

31. Monteith, J. L.; Unsworth, M. H. *Principle of Environmental Physics*, Second edition. Edward Arnold, London, 1990.

32. Belcher, S. E.; Jerram, N.; Hunt, J.C.R. Adjustment of a turbulent boundary layer to a canopy roughness elements. *J. Fluid Mech.* **2003**, *488*, 369–398.

33. Cionco, R. M. A preliminary model for air flow in the vegetative canopy. *Bull. Amer. Meteorl. Soc.* **1962**, *43*, 319.

34. Cionco. R. M.; Ohmsted, W. D.; Appleby, J. F. *A model for wind flow in an idealized vegetative canopy.* USAERDAA, Fort Huachuca, AZ, Meteorological Research Notes No. 5, ERDAA-MET-7-63, 1963.

Acronyms and Abbreviations

ARL	U.S. Army Research Laboratory
3DWF	3-dimensional wind field
JD	Julian date
LAI	leaf area index
LLJ	lower-level jet
m	meter
MO	Monin-Obukhov
NW	northwest
rms	root-mean-square
RSL	roughness sublayer
SE	southeast
SODAR	Sonic Detection and Ranging
UTC	Universal Time Coordinated
WIND	Wind in Non-uniform Domains

Distribution List

No. of Copies	Organization
pdf	ADMNSTR DEFNS TECHL INFO CTR DTIC-OCP (ELECTRONIC COPY) 8725 JOHN J KINGMAN RD STE 0944 FT BELVOIR VA 22060-6218
1 HC	DARPA ATTN IXO S WELBY 3701 N FAIRFAX DR ARLINGTON VA 22203-1714
1 HC	MIL ASST FOR ENV SCI OFC OF THE UNDERSEC OF DEFNS FOR RSRCH & ENGRG R&AT E LS PENTAGON RM 3D129 WASHINGTON DC 20301-3080
1 HC	OFC OF THE SECY OF DEFNS ATTN ODDRE (R&AT) THE PENTAGON WASHINGTON DC 20301-3080
1 HC	US ARMY TRADOC BATTLE LAB INTEGRATION & TECHL DIRCTRT ATTN ATCD B 10 WHISTLER LANE FT MONROE VA 23651-5850
1 HC	US ARMY CORPS OF ENGRS ENGR TOPOGRAPHICS LAB ATTN CETEC TR G P F KRAUSE 7701 TELEGRAPH RD ALEXANDRIA VA 22315-3864
1 HC	US ARMY CECOM INFOR & INTLLGNC WARFARE DIRCTRT ATTN AMSEL RD IW IP FT MONMOUTH NJ 07703-5211
1 HC	NATICK SOLIDER SYS COMMAND ATTN MAJ T STARK NATICK MA 01760
1 HC	SCI & TECHNLGY CORP 10 BASIL SAWYER DR HAMPTON VA 23666-1293
1 HC	SMC/GPA 2420 VELA WAY STE 1866 EL SEGUNDO CA 90245-4659
1 HC	TECOM ATTN CSTE DTC CL APG MD 21005-5057
1 HC	US ARMY CRREL ATTN CECRL GP M MORAN 72 LYME RD HANOVER NH 03755-1290
1 HC	US ARMY CRREL ATTN CERCL SI E L ANDREAS 72 LYME RD HANOVER NH 03755-1290
1 HC	US ARMY CRREL ATTN CRREL GP R DETSCH 72 LYME RD HANOVER NH 03755-1290
1 HC	US ARMY DUGWAY PROVING GROUND METEOROLOGY DIV ATTN J BOWERS WEST DESERT TEST CENTER DUGWAY UT 84022-5000
1 HC	US ARMY INFO SYS ENGRG CMND ATTN AMSEL-IE-TD F JENIA FT HUACHUCA AZ 85613-5300
1 HC	US ARMY MISSILE CMND ATTN AMSMI REDSTONE ARSENAL AL 35898-5243
1 HC	US ARMY NATICK RDEC ACTING TECHL DIR ATTN SBCN TP P BRANDLER KANSAS STREET BLDG 78 NATICK MA 01760-5056

No. of Copies	Organization
1 HC	US ARMY OEC ATTN CSTE AEC FSE 4501 FORD AVE PARK CENTER IV ALEXANDRIA VA 22302-1458
1 HC	COMMANDER US ARMY RDECOM ATTN AMSRD AMR W C MCCORKLE 5400 FOWLER RD REDSTONE ARSENAL AL 35898-5000
1 HC	US ARMY RSRCH DEV & ENG CMND SYSTEMS OF SYSTEMS INTEGRATION ATTN AMSRD SS T 6000 6TH STREET, SUITE 100 FT BELVOIR VA 22060-5608
2 HCs	US ARMY RSRCH LAB ATTN AMSRD ARL CI OK TP TECHL LIB T LANDFRIED BLDG 4600 APG MD 21005-5066
1 HC	US ARMY RSRCH LAB ATTN AMSRD ARL SL BB D HISLEY APG MD 21005-5066
1 HC	US ARMY RSRCH LAB ATTN STEWS IM IT TECHL LIB WSMR NM 88002
1 HC	US ARMY TOPO ENGR CTR ATTN CETEC ZC 1 FT BELVOIR VA 22060-5546
1 HC	US ARMY TRADOC ANAL CMND WSMR ATTN ATRC WSS R WSMR NM 88002-5502
1 HC	NAV AIR WAR CTR WPN DIV ATTN CMD 420000D C0245 A SHLANTA 1 ADMIN CIR CHINA LAKE CA 93555-6001

No. of Copies	Organization
1 HC	NAV POSTGRADUATE SCHL DEPT OF METEOROLOGY ATTN P FREDERICKSON 1 UNIVERSITY CIR MONTEREY CA 93943-5001
1 HC	NAV SURFC WEAPONS CTR ATTN CODE G63 DAHLGREN VA 22448-5000
1 HC	AFCCC/DOC ATTN GLAUBER 151 PATTON AVE RM 120 ASHEVILLE NC 28801-5002
1 HC	AIR FORCE ATTN WEATHER TECHL LIB 151 PATTON AVE RM 120 ASHEVILLE NC 28801-5002
1 HC	HDQTRS AFWA/DNX 106 PEACEKEEPER DR STE 2N3 OFFUTT AFB NE 68113-4039
1 HC	USAF ROME LAB TECH ATTN CORRIDOR W STE 262 RL SUL 26 ELECTR PKWY BLDG 106 GRIFFISS AFB NY 13441-4514
1 HC	DIRECTOR US ARMY RSRCH LAB ATTN AMSRD ARL RO EV W D BACH PO BOX 12211 RESEARCH TRIANGLE PARK NC 27709
1 HC	US ARMY RSRCH LAB ATTN AMSRD ARL CI COMP & INFO SCI DIR WSMR NM 88002-5501
1 HC	US ARMY RSRCH LAB ATTN SFAE C3T IE MET BLDG 1622 RM 131 WSMR NM 88002-5501

No. of Copies	Organization
1 HC	US ARMY RSRCH LAB ATTN AMSRD ARL CI EM D KNAPP BATTLEFIELD ENVIR DIRCTRT BLDG 1622 WSMR NM 88002-5501
1 HC	US ARMY RSRCH LAB ATTN AMSRD ARL CI EM D HOOCK BATTLEFIELD ENVIR DIRCTRT BLDG 1622 WSMR NM 88002-5501
1 HC	US ARMY RSRCH LAB ATTN IMNE ALC IMS MAIL & RECORDS MGMT
1 HC	ATTN AMSRD ARL D J M MILLER
2 CDs	ATTN AMSRD ARL CI OK TL TECHL LIB
2 CDs	ATTN AMSRD ARL CI OK T TECHL PUB
1 HC	ATTN AMSRD ARL CI J GOWENS
15 HCs	ATTN AMSRD ARL CI EM Y WANG
1 HC	ATTN AMSRD ARL CI EM R CIONCO
1 HC	ATTN AMSRD ARL CI E P CLARK
1 HC	ATTN AMSRD ARL CI ES J M NOBLE
1 HC	ATTN AMSRD ARL SE EA M SCANLON
1 HC	ATTN AMSRD ARL SE S J EICKE
1 HC	ATTN AMSRD ARL SE SA N SROUR
1 HC	ATTN AMSRD ARL SE SA S TENNEY ADELPHI MD 20783-1197
TOTAL:	68 (63 HCs, 4 CDs, 1 electronic)

INTENTIONALLY LEFT BLANK